Supplementary Information

Leveraging and understanding exotherms in tandem catalysts with *in situ* luminescence thermometry

Sinhara M.H.D. Perera[1], Benjamin Harrington[2], Adel Fadhul[1], Andrea D. Pickel[3*], and Marc D. Porosoff[1*]

[1]Department of Chemical and Sustainability Engineering, University of Rochester, Rochester, NY 14627, USA

[2]Materials Science Program, University of Rochester, NY 14627, USA

[3]Department of Mechanical Engineering, University of Rochester, Rochester, NY 14627, USA

Table of Contents

1. Materials and Catalyst Synthesis

Nitrogen (N_2) with ultra-high purity (99.999%) is obtained from Airgas. Isotopic gas mixtures of 10% v/v $^{13}CO_2/N_2$ (99 atom% isotopic purity), 10% v/v $^{12}CO_2/N_2$ and 9% v/v ^{12}CO/4.5% v/v O_2/ balance in N_2 are also sourced from Airgas. Tetraammineplatinum(II) nitrate (TAPN) (99.99% metal basis) and calcium nitrate tetrahydrate are purchased from ThermoFisher. Cerium(IV) oxide, CeO_2 (surface area: 30-50 $m^2\ g^{-1}$) is obtained from Alfa Aesar. The choice of TAPN is supported by prior literature, as multiple studies have shown it to be an effective Pt precursor across different synthesis routes, producing active and stable Pt/CeO_2 catalysts for CO oxidation.[1, 2] Upconverting nanoparticles (UCNPs) composed of $NaYF_4$: 20 at% Yb^{3+}, 2 at% Er^{3+} dispersed in cyclohexane are purchased from CD Bioparticles.

Pt-CaO/CeO_2, consisting of 1.5 wt% Pt and 15 wt% CaO supported on CeO_2, is synthesized via co-impregnation of tetraammineplatinum(II) nitrate and calcium nitrate tetrahydrate on CeO_2 through the incipient wetness impregnation (IWI) method. The impregnated material is dried at 60 °C for 12 hours, followed by calcination in air at 550 °C for 6 hours in a box furnace (Lindberg Blue M) with a ramp rate of 2 °C min^{-1}. Pt/CeO_2 (1.5 wt% Pt supported on CeO_2) and CaO/CeO_2 (15 wt% CaO supported on CeO_2) are synthesized similarly. To prepare UCNP-Pt-CaO/CeO_2, $NaYF_4$: Yb^{3+}, Er^{3+} is impregnated onto the Pt-CaO/CeO_2 via IWI with cyclohexane and dried at room temperature. Similarly, UCNP-Pt/CeO_2 and UCNP-CaO/CeO_2 are synthesized via the same impregnation method as the Pt-CaO DFM.

2. *In Situ* DRIFTS Isotopic Labeling Experiments

DRIFTS measurements are performed using a Nicolet iS50 spectrometer (Thermo Scientific) equipped with a liquid nitrogen-cooled MCT/A detector. To obtain DRIFTS spectra of isotopic CO_2/N_2 gas mixtures referenced to pure N_2 background, approximately 50 mg of spectroscopic-grade KBr is loaded into a Harrick Praying Mantis™ DRIFTS cell fitted with ZnSe windows. The cell is purged with N_2 (10 mL min^{-1}) at 25 °C for 15 minutes, and a background spectrum (BG 1) is recorded under this N_2 atmosphere. Subsequently, the isotopic CO_2/N_2 mixture (10 mL min^{-1}) is introduced into the cell, and the system is allowed to equilibrate for 30 minutes. Following equilibration, a sample spectrum referenced to BG 1 is collected.

To investigate CO_2 evolution during CO oxidation, approximately 50 mg of the Pt-CaO/CeO_2 sample is loaded into the DRIFTS cell. N_2 (10 mL min^{-1}) is flowed over the sample at

25 °C, and after 15 minutes of purging, a background spectrum (BG 2) is collected under N_2 prior to pretreatment. The sample is then heated to 400 °C at a rate of 10 °C min^{-1} and held at this temperature for 1 hour under continuous N_2 flow to remove pre-adsorbed CO_2. Afterward, the sample is cooled to 25 °C at the same ramp rate under N_2, and a post-pretreatment background spectrum (BG 3) is collected at 25 °C. Following pretreatment, the gas flow is switched to $^{13}CO_2/N_2$ (10 mL min^{-1}) to adsorb $^{13}CO_2$ at 25 °C. A series scan referenced to the BG 3 is collected during this process (99 scans per measurement, ~1 min per scan, data spacing: 0.482 cm^{-1}) until saturation of the surface is observed. The gas flow is then switched back to N_2 (10 mL min^{-1}), and the temperature is ramped to 150 °C at 10 °C min^{-1}. Once at temperature, a background spectrum (BG 4) is collected under N_2. A series scan referenced to BG 4 is acquired at 150 °C until the system reaches equilibrium and no gas-phase $^{13}CO_2$ remains. At this point, a new background (BG 5) is collected, and the gas flow is simultaneously switched to a reactive gas mixture of 9 vol% ^{12}CO/4.5 vol% O_2/ balance N_2 to initiate the CO oxidation reaction. A series of time-resolved spectra referenced to BG 5 is acquired continuously for 30 minutes.

3. Quantitative Energy Analysis of CO oxidation-driven CO_2 Evolution

To investigate the feasibility of thermally integrating CO oxidation with CO_2 desorption, a series of comparative experiments is performed with and without pre-adsorbed CO_2 on Pt-CaO/CeO_2. The reactions are carried out isothermally at 100 °C in a 1 mm quartz capillary reactor mounted within our custom-designed Clausen cell. The reaction temperature of 100 °C is selected based on temperature programmed reaction (TPR) results to maintain CO conversion below 1%, ensuring that the amount of CO_2 generated during the reaction remains on the same order of magnitude as the pre-adsorbed CO_2. At higher conversions, the much larger amount of CO_2 produced via CO oxidation becomes convoluted with the CO_2 desorption signal, such that we cannot close a mass balance and quantify the amount of pre-adsorbed CO_2 desorbing from the surface. Our methodology follows a sequence of four experiments detailed as follows: Approximately 2 mg of Pt-CaO/CeO_2 is loaded into a 1 mm ID quartz capillary reactor and connected to the Clausen cell. The system is first purged at 25 °C with N_2 at a flow rate of 10 mL min^{-1} and degassed by heating to 400 °C at a ramp rate of 10 °C min^{-1}, then holding for 1 hour under N_2. After degassing, the reactor is cooled to 100 °C (10 °C min^{-1}), and temperature and CO_2 concentration are recorded. After 5 minutes at 100 °C under N_2, the sequence of experiment begins with **Run 1**: The gas feed

is switched to a reactive mixture of 9 vol% CO/4.5 vol% O_2/balance N_2. Recording continues for 20 minutes, after which the gas is switched back to N_2, and the reactor is cooled to 25 °C at 10 °C min^{-1}. **Run 2** follows a similar protocol, except that after degassing, the reactor is cooled to 25 °C (10 °C min^{-1}) and the catalyst is saturated with CO_2 by flowing 10% CO_2 in N_2 for 5 minutes. Physisorbed CO_2 is then removed by purging with N_2 while ramping to 100 °C (10 °C min^{-1}), and the system is held at temperature until the CO_2 concentration drops below 10 ppm to ensure complete removal of physisorbed CO_2. The reactive CO mixture is then introduced, and temperature and CO_2 signals are recorded. **Run 3** is identical to **Run 1** to confirm reproducibility and rule out deactivation. **Run 4** is a control experiment following the same procedure as **Run 2,** but omitting introduction of the reactive gas mixture. After the CO_2 concentration drops below 10 ppm at 100 °C to ensure removal of physisorbed CO_2, the temperature is ramped to 400 °C at 10 °C min^{-1} and held for 0.5 hour under N_2, during which the CO_2 desorption profile is recorded and used to quantify the total chemisorbed CO_2.

As shown in **Figure S1**, CO oxidation without pre-adsorbed CO_2 (**Runs 1 and 3**) exhibits consistent CO_2 evolution profiles, confirming that the catalyst does not deactivate during the experimental sequence. In contrast, the run with pre-adsorbed CO_2 (**Run 2**) displays a clear excess of CO_2 relative to **Run 1** and **Run 3**, providing evidence that the heat generated from CO oxidation directly drives CO_2 desorption from the CaO adsorbent. This conclusion is further supported by the ~30 second shift of the CO_2 front in **Run 2** compared to **Run 1** and **Run 3**. In **Run 2**, where CaO is pre-saturated with CO_2, the exothermic heat released from CO oxidation triggered immediate CO_2 desorption. In contrast, in **Run 1** and **Run 3** with the absence of pre-adsorbed CO_2, CO_2 generated in situ adsorbed onto CaO, which acts as a CO_2 sink until saturation resulting in the observed temporal delay in CO_2 detection.

The results of the mass-balance experiments in **Figure S1** are summarized in **Table S1**. The data in the table indicates that complete desorption of chemisorbed CO_2 from CaO ($N_{CO_2,\,total}$ = 0.192 μmol, **eqn S1**) via thermal treatment at 400 °C for 30 mins requires approximately 544.7 kJ μmol CO_2^{-1} of external heat (**Figure S2**). The reaction-driven desorption of CO_2 (S_{CO_2}= 0.05 μmol, **eqn S2**) accounts for ~27% of $N_{CO_2,\,total}$ by only expending 26.4 kJ μmol CO_2^{-1} (**Table S1**, **Figure S2-3**), representing ~7% of the total external energy input typically required for desorbing $N_{CO_2,\,total}$ from CaO. We hypothesize the significant decrease in externally applied heat arises from

thermally coupling exo- and endothermic elementary reaction steps (CO oxidation and CO_2 desorption) at the active site level.

The amount of CO_2 desorbed N_{CO_2}(in moles) is calculated from the exhaust CO_2 concentration measured by the LI-COR gas analyzer using **eqn S1**. The volumetric flow rate of the gas is assumed to remain constant during the experiment, as the CO_2 concentration in the exhaust remains below 100 ppm and CO conversion is less than 1%, minimizing any perturbation to the overall flow. Energy consumption during CO_2 evolution is determined by integrating the area under the power-versus-time curve obtained from the Omega PID temperature controller. The total amount of chemisorbed CO_2 is calculated following **eqn S1** with the limits 0 to 60 mins. An upper limit of 60 minutes is selected, as the CO_2 concentration reaches equilibrium at this point (**Figure S1**). The fraction of CO_2 desorbed solely due to the heat released by the CO oxidation reaction, relative to the total amount of chemisorbed CO_2, S_{CO_2} is calculated according to **eqn S2**.

$$N_{CO_2} = \int_0^{1200} \nu_O \frac{P}{RT} x_{CO_2}\, dt \qquad \textbf{eqn S1}$$

Where, ν_o represents the volumetric gas flow rate ($m^3\ s^{-1}$), P is the pressure at the gas analyzer cell (Pa), T is the temperature at the gas analyzer cell (K), R is the universal gas constant (J mol K^{-1}), x_{CO_2} is mole fraction CO_2 in the exhaust gas, and t is time (s).

$$S_{CO_2} = \frac{N_{CO_{2,\,run2}} - \frac{1}{2}\left(N_{CO_{2,\,run1}} + N_{CO_{2,\,run3}}\right) - N_{CO_{2,\,run4}}}{N_{CO_{2,\,total}}} \times 100\% \qquad \textbf{eqn S2}$$

Where, $N_{CO_{2,\,runi}}$is the number of CO_2 moles desorbed during i^{th} run of the sequence and $N_{CO_{2,\,total}}$is the total chemisorbed CO_2 at 100 °C.

4. Working Principle of Ratiometric Luminescence Thermometry

UCNPs are inorganic luminescent probes typically composed of fluoride or oxide host lattices doped with multiple lanthanide ions. In $NaYF_4$ co-doped with Yb^{3+} and Er^{3+}, Yb^{3+} functions as a sensitizer that is responsible for absorption of near-infrared light. Energy is then transferred from Yb^{3+} to the activator, Er^{3+}, which ultimately emits shorter wavelength visible light. Yb^{3+} ions exhibit strong absorption at 976 nm, promoting electrons from the $^2F_{7/2}$ ground state to the $^2F_{5/2}$ excited state. Excited Yb^{3+} ions then transfer energy to a nearby Er^{3+} ion in a two-photon

upconversion process, exciting Er^{3+} to its $^4F_{7/2}$ state, which rapidly relaxes non-radiatively to the $^2H_{11/2}$ and $^4S_{3/2}$ states (**Figure S4**). Subsequently, radiative relaxation from these states to the ground state ($^4I_{15/2}$) occurs, resulting in emission of green luminescence.[3, 4] The $^2H_{11/2}$ and $^4S_{3/2}$ levels of Er^{3+} are thermally coupled, separated by a small energy gap (~0.1 eV),[5] with their relative populations governed by Boltzmann statistics. The UCNP thermometry signal is determined from the luminescence intensity ratio *r*, which is defined as the ratio of the integrated emission intensity over wavelength ranges corresponding to the two transitions, as described in **eqn S3**.

$$r \equiv \frac{\int_{513}^{535} I_\lambda \, d\lambda}{\int_{535}^{548} I_\lambda \, d\lambda} = A \, exp\left(-\frac{\Delta E}{k_B T}\right) \qquad \textbf{eqn S3}$$

The variables in **eqn S3** are as follows: I_λ is the emission intensity, ΔE is the energy gap between the $^2H_{11/2}$ and $^4S_{3/2}$ levels, k_B is the Boltzmann constant, and A is a proportionality constant that accounts for the radiative transition probabilities from $^2H_{11/2}$ and $^4S_{3/2}$ to the ground state $^4I_{15/2}$.

5. Characterization

Transmission electron microscopy (TEM) is performed using a FEI Tecnai G2-F20 STEM operated at 200 kV. Dry powder samples are deposited onto carbon-coated copper grids without any additional pretreatment before insertion into the TEM chamber.

Scanning electron microscopy (SEM) is carried out using a Zeiss Auriga microscope equipped with a Schottky field emission gun, operated at 20.00 kV with a working distance of 5.1 mm. Energy-dispersive X-ray spectroscopy (EDX) is performed using an EDAX Octane Elect Plus detector integrated into the SEM, featuring a silicon drift detector.

6. Optical Setup for UCNP-Based Luminescence Thermometry

Optical measurements are carried out using a custom-built confocal microscopy and spectroscopy system. Excitation is provided by a continuous-wave 976 nm fiber-coupled diode laser (BL976-PAG500, Thorlabs), filtered through a 975/10 nm bandpass filter (LD01-975/10-25, Semrock). A high-numerical aperture (NA = 0.7) 100× dry air objective lens (Mitutoyo Plan Apo NIR HR) is used to focus the laser beam on the sample. A 775 nm shortpass dichroic mirror (zt775sp-2p-uf3, Chroma) is employed to reflect the excitation beam toward the sample while allowing the

upconverted emission to pass through. Emission is further filtered using a 785 nm shortpass filter (BSP01-785R-25, Semrock) to remove residual excitation light before being directed into a spectrometer (Andor Kymera 193i) equipped with an iDus 420 CCD detector for spectral acquisition. For the temperature calibration (**Figure S7**), a precision thermal stage (custom-modified HCS321Gi, Instec) is used to conduct measurements from room temperature up to the maximum achievable temperature for the stage of 250 °C, which is only marginally below the maximum temperature measured during CO oxidation of ~280 °C.

7. *In Situ* Luminescence Thermometry during CO Oxidation

2 mg of UCNP-Pt-CaO/CeO_2 is loaded into a quartz capillary reactor and connected to the Clausen cell apparatus. The system is purged at 25 °C with N_2 at a flow rate of 10 mL min^{-1} until the CO_2 concentration drops below 10 ppm (CO_2 concentration is monitored by LI-COR (LI-850) gas analyzer). Once stabilized, temperature and CO_2 concentration recordings are simultaneously started. N_2 flow is maintained for an additional 5 minutes at 25 °C, after which the feed is switched to a reactive gas mixture consisting of 9 vol% CO/4.5 vol% O_2/balance N_2. This mixture is flowed for 15 minutes at 25 °C prior to initiating the TPR, which proceeds as follows:

1. Ramp to 125 °C at 10 °C min^{-1} and hold for 5 minutes
2. Ramp to 150 °C at 10 °C min^{-1} and hold for 5 minutes
3. Ramp to 170 °C at 10 °C min^{-1}

To probe the effect of DFM component proximity on thermal coupling, analogous experiments are performed with pre-adsorbed CO_2 on both the co-impregnated DFM (2 mg) and a dual-bed DFM comprising UCNP-Pt/CeO_2 and UCNP-CaO/CeO_2. In the dual-bed configuration, each portion of the DFM (2 mg) is packed between quartz wool plugs, with an additional quartz wool layer separating the two beds. From inlet to outlet, the reactor is packed in the following sequence: quartz wool, UCNP-Pt/CeO_2, quartz wool, UCNP-CaO/CeO_2, quartz wool. Pre-adsorption of CO_2 is carried out by flowing a 10% CO_2/N_2 mixture (10 mL min^{-1}) for 5 min at 25 °C. Physisorbed CO_2 is subsequently removed by purging with N_2 (10 mL min^{-1}) at 25 °C, after which the experiments are conducted following the same procedure as described above.

8. Proximity Effects on the Initial Rate of CO_2 Desorption

A DRIFTS experiment is conducted to compare the initial rate of CO_2 desorption concurrent with exothermic CO oxidation in co-impregnated versus dual-bed DFMs pre-adsorbed with isotopically labeled $^{13}CO_2$. DRIFTS measurements are performed on a Nicolet iS50 spectrometer (Thermo Scientific) equipped with a liquid nitrogen-cooled MCT/A detector. DFM samples (40 mg total) are loaded into a Harrick Praying Mantis™ DRIFTS cell fitted with ZnSe windows. For the dual-bed configuration, 20 mg of Pt/CeO_2 (bottom) and 20 mg of CaO/CeO_2 (top) are packed sequentially. The cell is first purged with N_2 (10 mL min^{-1}) for 15 min, followed by degassing under N_2 at 400 °C (10 °C min^{-1}) for 1 h, and subsequently cooled to 25 °C (10 °C min^{-1}). Pre-adsorption of $^{13}CO_2$ is achieved by flowing a 10% $^{13}CO_2/N_2$ mixture (10 mL min^{-1}) for 30 min at 25 °C. After saturation, the gas flow is switched to N_2 (10 mL min^{-1}), and the temperature is ramped to 150 °C (10 °C min^{-1}). Physisorbed $^{13}CO_2$ is removed by purging with N_2 at 150 °C for 30 min. Once equilibrated, a background spectrum is recorded under N_2, after which the reactive gas mixture (9 vol% ^{12}CO / 4.5 vol% O_2 / balance N_2, 10 mL min^{-1}) is introduced isothermally at 150 °C. Spectral acquisition is initiated simultaneously, with 99 scans per measurement (~1 min per scan, data spacing: 0.482 cm^{-1}), and referenced to the background spectrum. The following equations are used to determine the rate of $^{13}CO_2$ desorption (dC*/dt) from the DFM surface:

$$A_0 = \frac{A}{m.\beta} \qquad \textbf{eqn S4}$$

$$A_0 = \alpha C_* \qquad \textbf{eqn S5}$$

$$\frac{dA_0}{dt} = \alpha \frac{dC_*}{dt} \qquad \textbf{eqn S6}$$

Where A is the peak area of the P branch of CO_2 ν_3 band, A_0 is normalized peak area, m is the catalyst mass, β is peak-to-peak signal intensity, α is the extinction coefficient of $^{13}CO_2$ and C_* is the gas-phase concentration of $^{13}CO_2$.

9. Correlating Catalyst Surface Temperature in a DRIFTS Cell with Reaction Rate

The experimental setup consisted of a LI-COR gas analyzer connected to the exhaust of the DRIFTS cell of a Nicolet iS50 spectrometer. A 44 mg sample of co-impregnated Pt-CaO/γ-Al_2O_3 catalyst is loaded into the DRIFTS sample chamber. The cell is first purged with N_2 (10 mL min^{-}

$^{-1}$) for 15 min, followed by degassing under N_2 at 400 °C (10 °C min^{-1}) for 1 h, and subsequently cooled to 25 °C (10 °C min^{-1}). The temperature is then raised to 150 °C (10 °C min^{-1}) under N_2. Once stabilized at 150 °C, the reactive gas mixture (9 vol% CO / 4.5 vol% O_2 / balance N_2, 10 mL min^{-1}) is introduced isothermally, and the outlet CO_2 concentration is recorded. The reaction rate is calculated using **eqn S7-12**.

For calibration of surface temperature versus reaction rate, a 115 mg catalyst sample diluted with KBr at a 1:10 wt% catalyst-to-KBr ratio is loaded into the sample chamber and degassed following the same pretreatment. The reactive gas mixture at 10 mL min^{-1} is introduced at 25 °C and allowed to equilibrate for 30 min prior to initiating the following temperature program, during which outlet CO_2 concentration is continuously monitored. The average rate at each isothermal step was then used to generate the calibration curve (**Figure S13**). For improved accuracy, the calibration curve is plotted only over the 150-250 °C range.

1. Ramp to 100 °C (10 °C min^{-1}) and hold for 15 min
2. Ramp to 125 °C (10 °C min^{-1}) and hold for 15 min
3. Ramp to 150 °C (10 °C min^{-1}) and hold for 15 min
4. Ramp to 175 °C (10 °C min^{-1}) and hold for 15 min
5. Ramp to 200 °C (10 °C min^{-1}) and hold for 15 min
6. Ramp to 225 °C (10 °C min^{-1}) and hold for 15 min
7. Ramp to 250 °C (10 °C min^{-1}) and hold for 15 min
8. Ramp to 275 °C (10 °C min^{-1}) and hold for 15 min
9. Ramp to 300 °C (10 °C min^{-1}) and hold for 15 min

$$\dot{n}_{out} = \dot{n}_{out,N2} + \dot{n}_{out,O2} + \dot{n}_{out,CO} + \dot{n}_{out,CO2} \quad \textbf{eqn S7}$$

$$\dot{n}_{out} = \dot{n}_{in,N2} + (n_{in,O2} - \frac{\dot{n}_{out,CO2}}{2}) + (n_{in,CO} - \dot{n}_{out,CO2}) + \dot{n}_{out,CO2} \quad \textbf{eqn S8}$$

$$\dot{n}_{out} = \dot{n}_{in} + \frac{\dot{n}_{out,CO2}}{2} \quad \textbf{eqn S9}$$

$$\dot{n}_{out,CO2} = \dot{n}_{out}\, x_{out,CO2} \quad \textbf{eqn S10}$$

$$\dot{n}_{out,CO2} = \dot{n}_{in}\left(\frac{2\, x_{out,CO2}}{2 - x_{out,CO2}}\right) \quad \textbf{eqn S11}$$

$$Rate = \frac{\dot{n}_{out,CO2}}{m}$$ **eqn S12**

Where, $\dot{n}_{out}$ is the total outlet molar flow rate, $\dot{n}_{out,i}$ is the outlet molar flow rate of species i, $\dot{n}_{in,i}$ is the inlet molar flow rate of species i, $\dot{n}_{in}$ is the total inlet molar flow rate, $x_{out,CO2}$ is the outlet CO_2 mole fraction, and m is the active catalyst mass.

10. Figures

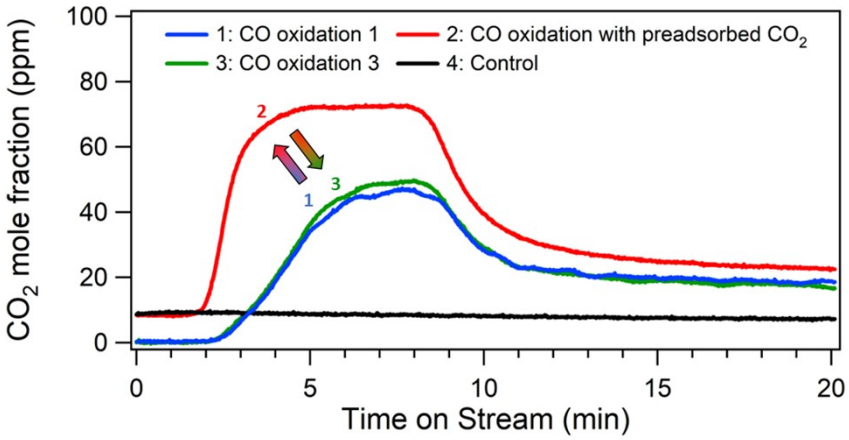

Figure S1: Quantitative analysis of CO_2 evolution during sequential CO oxidation experiments over Pt-CaO/CeO_2. Four sequential experimental runs are performed: **run 1** (blue): CO oxidation without pre-adsorbed CO_2; **run 2** (red): CO oxidation with pre-adsorbed CO_2; **run 3** (green): repeat of run 1 to verify reproducibility and rule out catalyst deactivation; and **control** (black): conducted under N_2 to establish a non-reactive baseline. Time on stream denotes time after beginning the CO oxidation reaction.

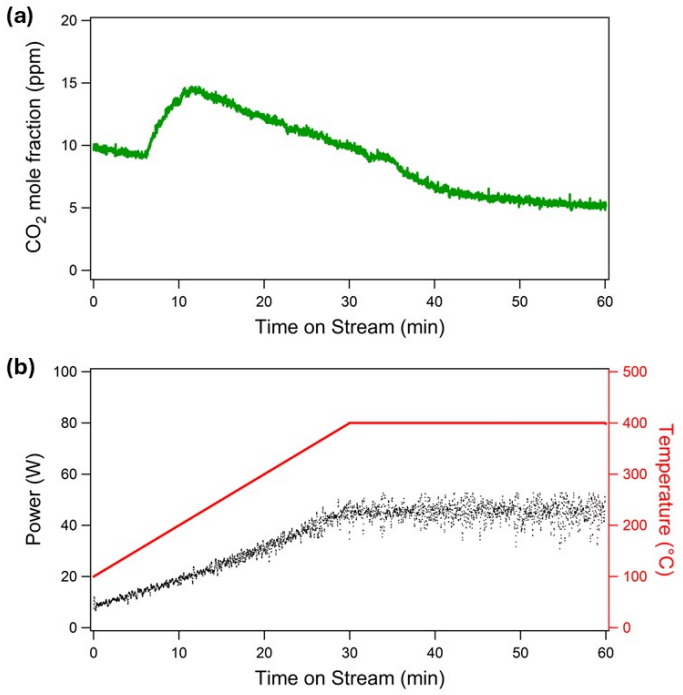

Figure S2: Quantification of total chemisorbed CO_2 and associated energy consumption. **(a)** CO_2 desorption profile following the removal of physisorbed CO_2 at 100 °C, measured during ramping to 400 °C and holding for 0.5 hours under N_2. **(b)** Corresponding power versus time curve used to calculate total energy consumption.

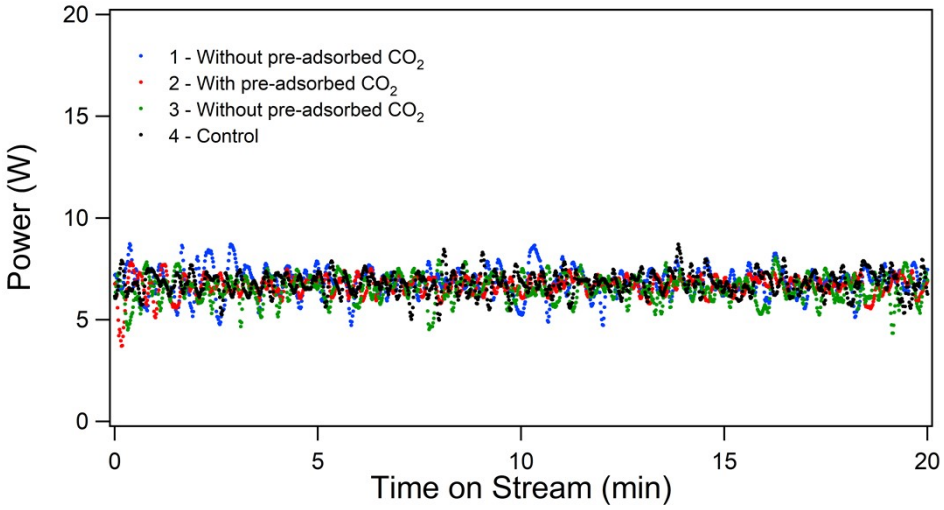

Figure S3: Power consumption during sequential CO oxidation experiments over Pt-CaO/CeO_2. Four sequential experimental runs are performed: run 1 (**blue**): CO oxidation without pre-adsorbed CO_2; run 2 (**red**): CO oxidation with pre-adsorbed CO_2; run 3 (**green**): repeat of run 1 to verify reproducibility and rule out catalyst deactivation; and control (**black**): conducted under N_2 to establish a non-reactive baseline.

Table S1: Quantitative analysis of energy required to drive CO_2 desorption by the heat released from CO oxidation. All experiments are sequential and use 2 mg of DFM loaded into the reactor.

Run	CO_2 Released (µmol)	Energy (kJ)	Desorption Efficiency (kJ µmol CO_2^{-1})
(1) Without pre-adsorbed CO_2	0.187	8.2	43.9
(2) With pre-adsorbed CO_2	0.304	8.0	26.4
(3) Without pre-adsorbed CO_2 (repeat of 1)	0.177	7.8	44.1
(4) Control under N_2	0.069	8.2	119.2
Total chemisorbed CO_2 ($N_{CO_{2,total}}$)	0.192	88.6	544.7

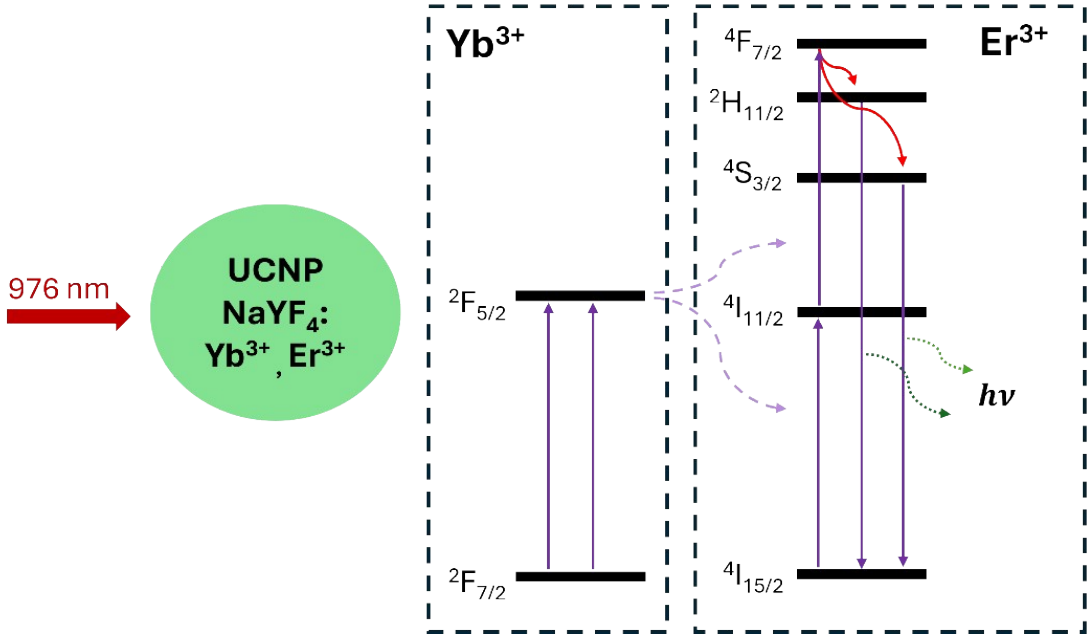

Figure S4: Energy transfer and upconversion mechanism in $NaYF_4$: Yb^{3+}, Er^{3+} UCNPs.

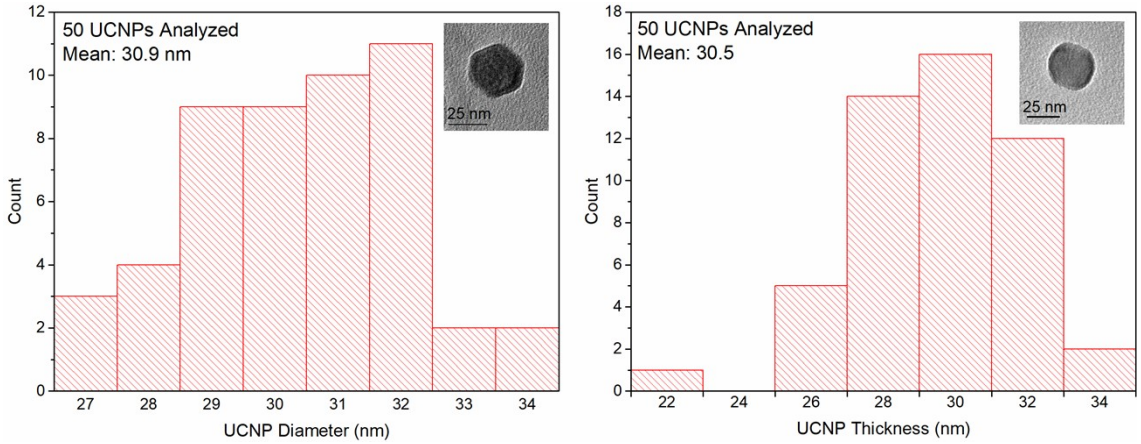

Figure S5: Particle size analysis performed using TEM images of UCNPs. Each histogram consists of 50 different UCNPs. **(a)** Distribution of UCNP diameters, defined as the distance across the hexagonally shaped facet. **(b)** Distribution of UCNP thicknesses, measured as the distance between the two hexagonal faces. Insets provide representative orientations of UCNPs.

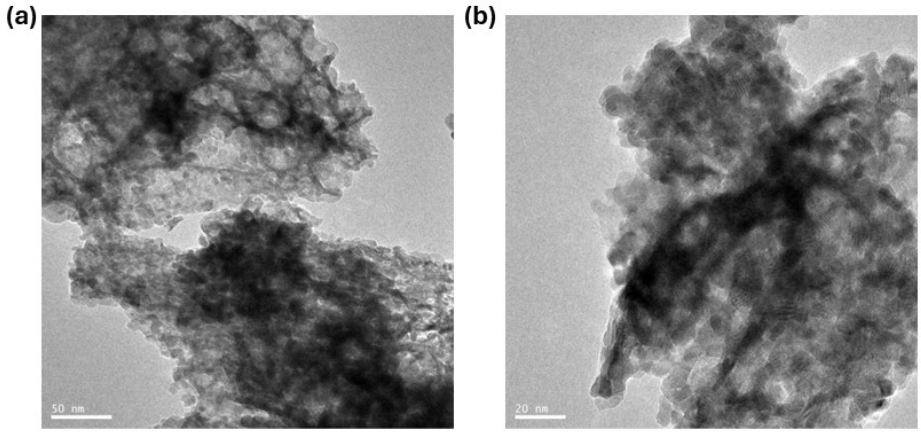

Figure S6: TEM images highlighting the uniform dispersion of Pt nanoparticles, **(a)** 50 nm and **(b)** 20 nm scales.

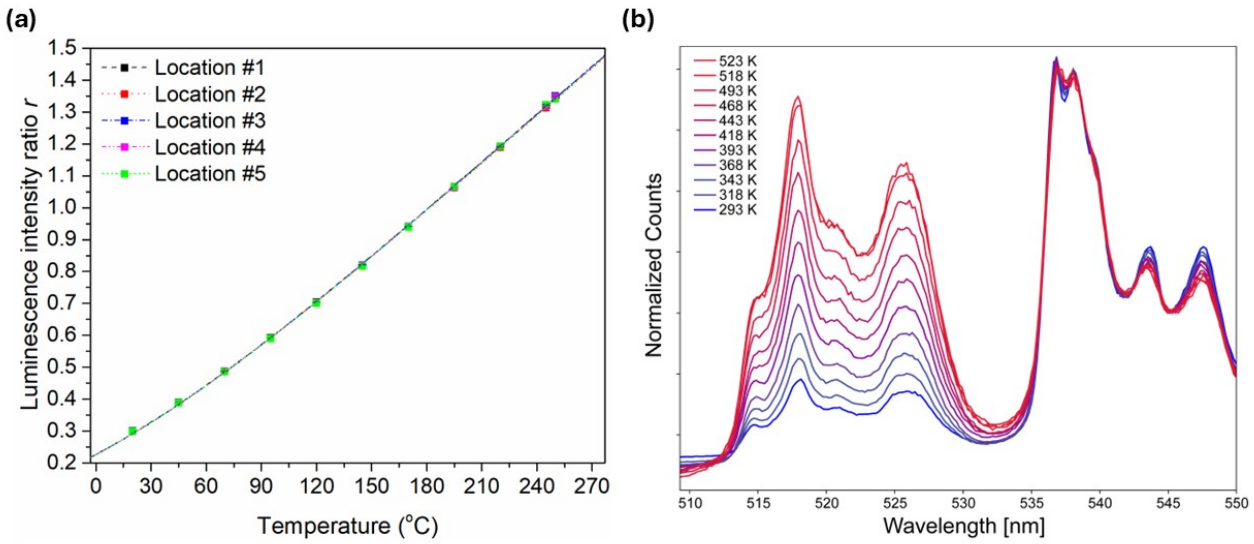

Figure S7: (a) Ratiometric luminescence thermometry calibration acquired across 5 locations of UCNPs dispersed on a glass substrate. The temperature calibration is performed using a thermal stage with a maximum temperature limit of approximately 250 °C. **(b)** Representative temperature-dependent UCNP spectra, used to acquire the temperature calibration shown in (a).

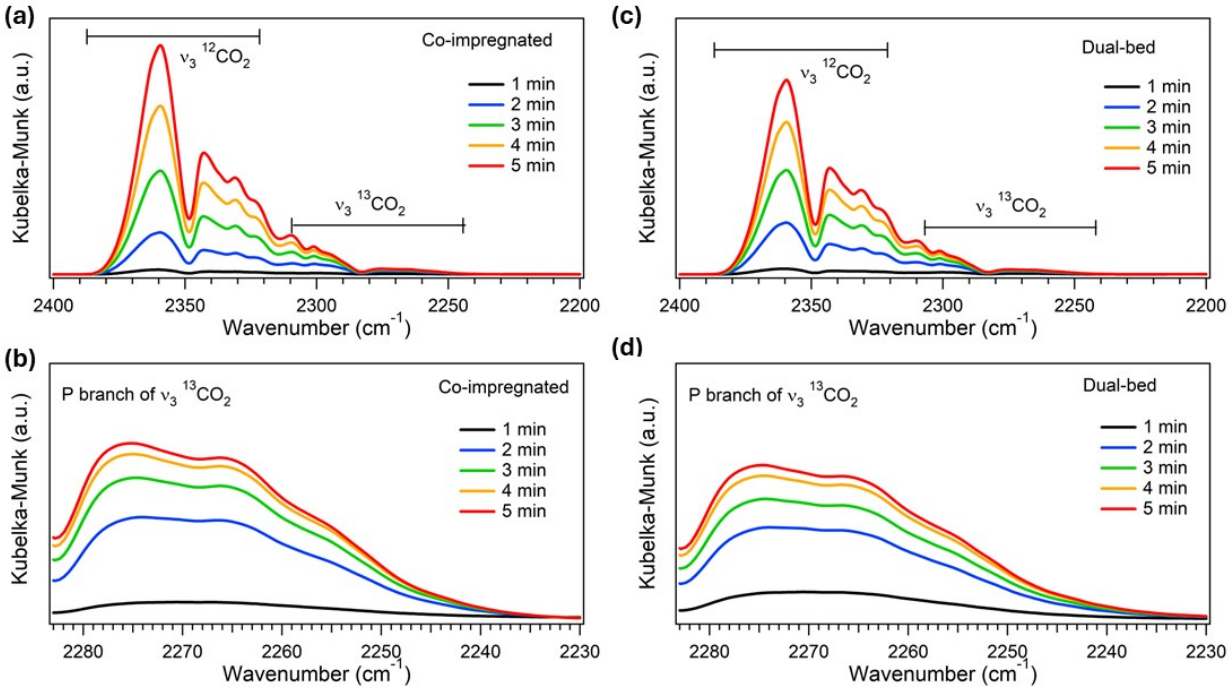

Figure S8: DFM component proximity effects on the initial rate of $^{13}CO_2$ desorption. **(a)** Evolution of the $^{13}CO_2$ ν_3 and $^{12}CO_2$ ν_2 bands upon introduction of the reactive gas mixture (9 vol% ^{12}CO / 4.5 vol% O_2 / balance N_2, 10 mL min^{-1}) at 150 °C. **(b)** Zoomed-in evolution of the P branch of $13CO_2$ ν_3 band for the co-impregnated catalyst. **(c–d)** Corresponding plots for the dual-bed configuration.

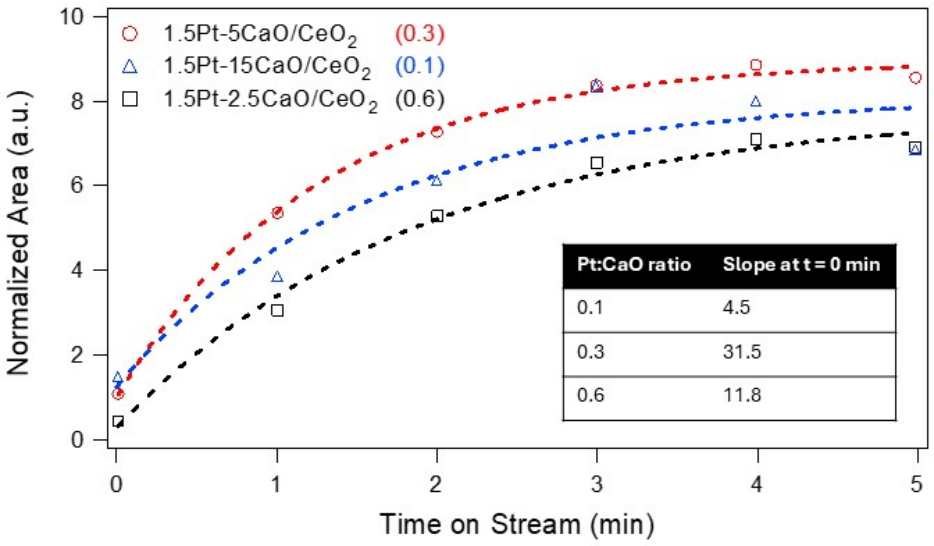

Figure S9: Comparison of the initial rate of $^{13}CO_2$ desorption during exothermic ^{12}CO oxidation at 150 °C for the co-impregnated catalyst with varying Pt:CaO mass ratio, measured by DRIFTS. The normalized area of the P-branch of the $^{13}CO_2$ ν_3 band (I_0) is plotted against time-on-stream under reaction conditions, and the initial rate of change of the peak area (dI_0/dt) is directly proportional to the initial rate of $^{13}CO_2$ desorption. The experimental data were fitted using an exponential function of the form $k_0 + k_1 \exp(-k_3 x)$, where k_0, k_1, and k_2 are constants.

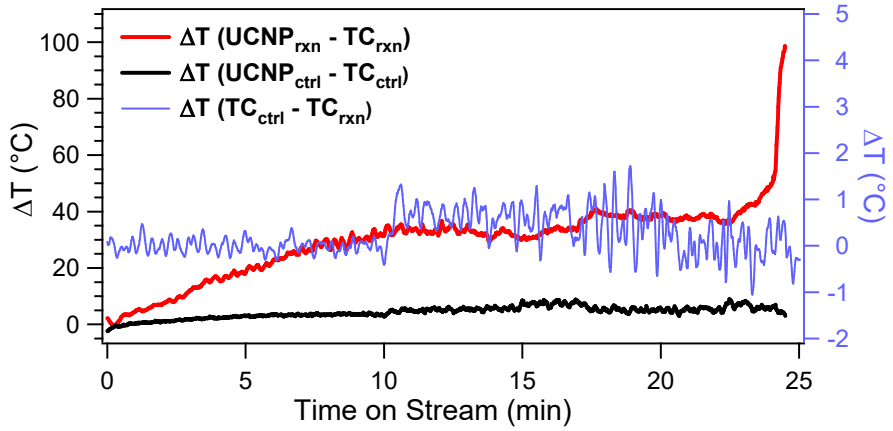

Figure S10: The temperature difference between the DFM surface and bed boundary highlights significant local thermal gradients induced by the exothermic reaction (left axis). The temperature difference between the thermocouple (TC) in contact with the DFM bed during the control experiment and reaction (right) are nearly identical and deviate < 2 °C for the entire experiment and < 1 °C for most of the experiment, with the exception of a short window around 18 minutes time on stream.

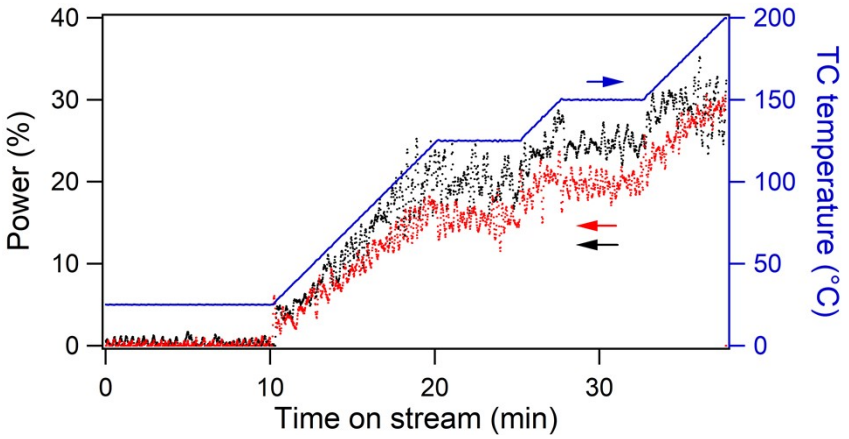

Figure S11: Power output by the temperature controller during thermocouple (TC) placement within the catalyst bed (black), and quartz wool (red). The TC temperature is included in blue as a reference.

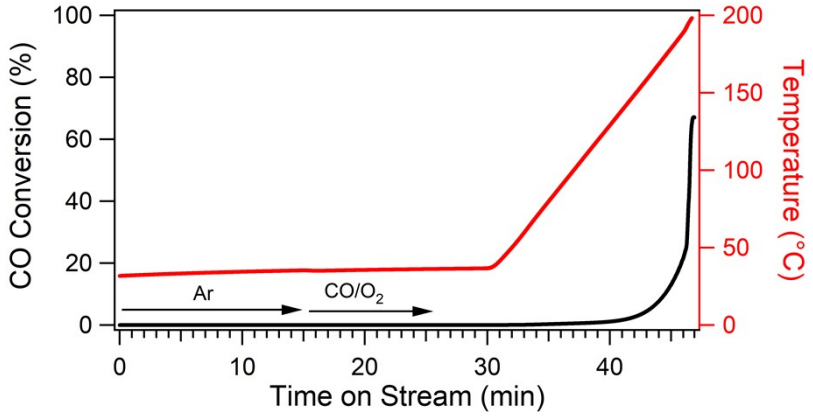

Figure S12: CO oxidation temperature-programmed reaction (TPR) over Pt-CaO/CeO_2 using a reactive gas mixture of 9 vol% CO/4.5 vol% O_2/balance N_2.

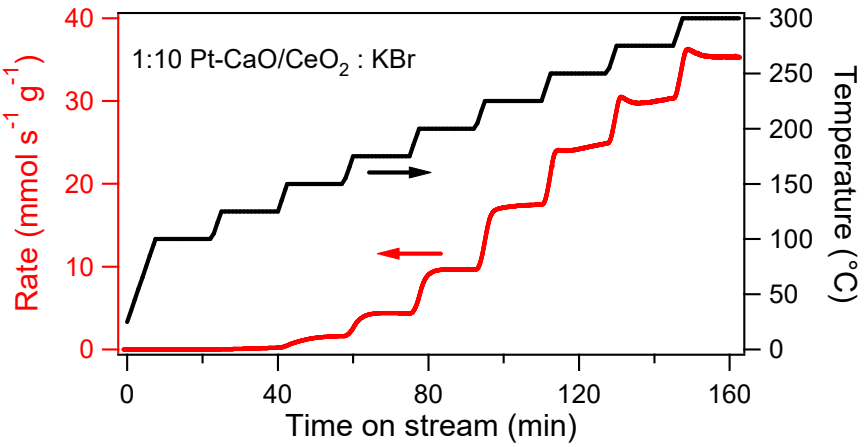

Figure S13: Raw data used to construct the surface temperature versus rate calibration curve for the co-impregnated DFM (Pt-CaO/CeO_2) shown in Figure 5c. The average rate at each isothermal step was used to generate the calibration curve.

11. References

(1) Zhang, Z.; Tian, J.; Lu, Y.; Yang, S.; Jiang, D.; Huang, W.; Li, Y.; Hong, J.; Hoffman, A. S.; Bare, S. R.; et al. Memory-dictated dynamics of single-atom Pt on CeO(2) for CO oxidation. *Nat Commun* **2023**, *14* (1), 2664. DOI: 10.1038/s41467-023-37776-3.

(2) Bohigues, B.; Rojas-Buzo, S.; Salusso, D.; Xia, Y.; Corma, A.; Bordiga, S.; Boronat, M.; Willhammar, T.; Moliner, M.; Serna, P. Overcoming activity/stability tradeoffs in CO oxidation catalysis by Pt/CeO(2). *Nat Commun* **2025**, *16* (1), 7451. DOI: 10.1038/s41467-025-62726-6.

(3) Fischer, L. H.; Harms, G. S.; Wolfbeis, O. S. Upconverting nanoparticles for nanoscale thermometry. *Angew Chem Int Ed Engl* **2011**, *50* (20), 4546-4551. DOI: 10.1002/anie.201006835.

(4) Shinn, M. D.; Sibley, W. A.; Drexhage, M. G.; Brown, R. N. Optical transitions ofEr3+ions in fluorozirconate glass. *Physical Review B* **1983**, *27* (11), 6635-6648. DOI: 10.1103/PhysRevB.27.6635.

(5) Hartman, T.; Geitenbeek, R. G.; Whiting, G. T.; Weckhuysen, B. M. Operando monitoring of temperature and active species at the single catalyst particle level. *Nature Catalysis* **2019**, *2* (11), 986-996. DOI: 10.1038/s41929-019-0352-1.